Research Article | Vol. 25, No. 7 | 3 Apr 2017 | OPTICS EXPRESS 8350
Optics EXPRESS

# Study of chromatic adaptation using memory color matches, Part II: colored illuminants

KEVIN A. G. SMET,[1*] QIYAN ZHAI,[2] MING R. LUO,[2,3] AND PETER HANSELAER[1]

[1]*ESAT/Light & Lighting Laboratory, KU Leuven, Ghent, Belgium*
[2]*State Key Laboratory of Modern Optical Instrumentation, Zhejiang University, Hangzhou, China*
[3]*m.r.luo@zju.edu.cn*
[*]*Kevin.Smet@kuleuven.be*

**Abstract:** In a previous paper, 12 corresponding color data sets were derived for 4 neutral illuminants using the long-term memory colours of five familiar objects. The data were used to test several linear (one-step and two-step von Kries, RLAB) and nonlinear (Hunt and Nayatani) chromatic adaptation transforms (CAT). This paper extends that study to a total of 156 corresponding color sets by including 9 more colored illuminants: 2 with low and 2 with high correlated color temperatures as well as 5 representing high chroma adaptive conditions. As in the previous study, a two-step von Kries transform whereby the degree of adaptation $D$ is optimized to minimize the $DE_{u'v'}$ prediction errors outperformed all other tested models for both memory color and literature corresponding color sets, whereby prediction errors were lower for the memory color set. Most of the transforms tested, except the two- and one-step von Kries models with optimized $D$, showed large errors for corresponding color subsets that contained non-neutral adaptive conditions as all of them tended to overestimate the effective degree of adaptation in this study. An analysis of the impact of the sensor space primaries in which the adaptation is performed was found to have little impact compared to that of model choice. Finally, the effective degree of adaptation for the 13 illumination conditions (4 neutral + 9 colored) was successfully modelled using a bivariate Gaussian in a Macleod-Boyton like chromaticity diagram.



**OCIS codes:** (330.0330) Vision, color, and visual optics; (330.4060) Vision modeling; (330.7320) Vision adaptation; (330.1720) Color vision; (330.5020) Perception psychology; (330.5510) Psychophysics.

## References and links

1. CIE160-2004, *A Review of Chromatic Adaptation Transforms* (CIE, 2004).
2. N. Moroney, M. D. Fairchild, R. W. G. Hunt, C. Li, M. R. Luo, and T. Newman, "The CIECAM02 color appearance model," in *IS&T/SID Tenth Color Imaging Conference* (2002), p. 23.
3. I. Kuriki, "The loci of achromatic points in a real environment under various illuminant chromaticities," Vision Res. **46**, 3055-3066 (2006).
4. D. B. Judd, "Hue saturation and lightness of surface colors with chromatic illumination," J. Opt. Soc. Am. **30**, 2-32 (1940).
5. K. A. G. Smet, Q. Zhai, M. R. Luo, and P. Hanselaer, "The study of chromatic adaptation using memory colors, Part I: neutral Illuminants," Opt. Express, in press (2017).
6. K. A. G. Smet, G. Deconinck, and P. Hanselaer, "Chromaticity of unique white in illumination mode," Opt. Express **23**, 12488-12495 (2015).
7. K. A. G. Smet, G. Deconinck, and P. Hanselaer, "Chromaticity of unique white in object mode," Opt. Express **22**, 25830-25841 (2014).
8. D. H. Foster, "Color constancy," Vision Res. **51**, 674-700 (2011).
9. J. Golz, "The role of chromatic scene statistics in color constancy: Spatial integration," J. Vis. **8**, 6-6 (2008).
10. M. D. Fairchild and L. Reniff, "Time-course of chromatic adaptation for color-appearance judgments," J. Opt. Soc. Am. A **12**, 824-833 (1995).
11. P. A. Garcia, R. Huertas, M. Melgosa, and G. Cui, "Measurement of the relationship between perceived and computed color differences," J. Opt. Soc. Am. A **24**, 1823-1829 (2007).
12. P. E. Shrout and J. L. Fleiss, "Intraclass correlations: Uses in assessing rater reliability," Psychol. Bull. **2**, 420-428 (1979).
13. M. D. Fairchild, *Color Appearance Models,* 2 ed. (John Wiley & Sons, 2005), p. 408.

#282729 https://doi.org/10.1364/OE.25.008350
Journal © 2017 Received 13 Dec 2016; revised 22 Feb 2017; accepted 19 Mar 2017; published 31 Mar 2017

Optics EXPRESS


14. S. Süsstrunk, J. Holm, and G. D. Finlayson, "Chromatic adaptation performance of different RGB sensors," in *IS&T/SPIE Electronic Imaging 2001: Color Imaging,* (San Jose, CA, 2001), pp. 172-183.
15. K. M. Lam, "Metamerism and colour constancy. Ph.D. thesis," (University of Bradford, 1985).
16. C. Li, M. R. Luo, B. Rigg, and R. W. G. Hunt, "CMC 2000 chromatic adaptation transform: CMCCAT2000," Color Res. Appl. **27**, 49-58 (2002).
17. S. Bianco and R. Schettini, "Two new von Kries based chromatic adaptation transforms found by numerical optimization," Color Res. Appl. **35**, 184-192 (2010).
18. R. W. G. Hunt, "Revised colour-appearance model for related and unrelated colours," Color Res. Appl. **16**, 146-165 (1991).
19. Y. Nayatani, K. Hashimoto, K. Takahama, and H. Sobagaki, "A nonlinear color-appearance model using Estévez-Hunt-Pointer primaries," Color Res. Appl. **12**, 231-242 (1987).
20. M. R. Luo and R. W. G. Hunt, "The structure of the CIE 1997 colour appearance model (CIECAM97s)," Color Res. Appl. **23**, 138-146 (1998).
21. L. Mori, H. Sobagaki, H. Komatsubara, and K. Ikeda, "Field trials on CIE chromatic adaptation formula," in *CIE 22nd Session* (Melbourne, 1991), pp. 55–58.
22. H. Helson, D. B. Judd, and M. H. Warren, "Object-color changes from daylight to incandescent filament illumination," J. Illum. Eng. **47**, 13 (1952).
23. M. R. Luo, A. A. Clarke, P. A. Rhodes, A. Schappo, S. A. R. Scrivener, and C. J. Tait, "Quantifying color appearance.1.LUTCHI color appearance data," Color Res. Appl. **16**, 166-180 (1991).
24. W. G. Kuo, M. R. Luo, and H. E. Bez, "Various chromatic-adaptation transformations tested using new color appearance data in textiles," Color Res. Appl. **20**, 313-327 (1995).
25. E. J. Breneman, "Corresponding chromaticities for different states of adaptation to complex visual-fields," J. Opt. Soc. Am. A **4**, 1115-1129 (1987).
26. K. M. Braun and M. D. Fairchild, "Psychophysical generation of matching images for cross-media color production," in *IS&T and SID's 4th Color Imaging Conference: Color Science, Systems, and Applications,* (IS&T, Springfield, Va, USA, 1996), pp. 214-220.
27. J. J. McCann, S. P. McKee, and T. H. Taylor, "Quantitative studies in retinex theory - comparison between theoretical predictions and observer responses to color Mondrian experiments," Vision Res. **16**, 445-& (1976).
28. M. R. Luo, G. Cui, and B. Rigg, "The development of the CIE 2000 colour-difference formula: CIEDE2000," Color Res. Appl. **26**, 340-350 (2001).
29. K. A. G. Smet, Y. Lin, B. V. Nagy, Z. Németh, G. L. Duque-Chica, J. M. Quintero, H.-S. Chen, R. M. Luo, M. Safi, and P. Hanselaer, "Cross-cultural variation of memory colors of familiar objects," Opt. Express **22**, 32308-32328 (2014).
30. M. Melgosa, P. A. García, L. Gómez-Robledo, R. Shamey, D. Hinks, G. Cui, and M. R. Luo, "Notes on the application of the standardized residual sum of squares index for the assessment of intra- and inter-observer variability in color-difference experiments," J. Opt. Soc. Am. A **28**, 949-953 (2011).
31. H. Wang, G. Cui, M. R. Luo, and H. Xu, "Evaluation of colour-difference formulae for different colour-difference magnitudes," Color Res. Appl. **37**, 316-325 (2012).
32. M. S. Rea and J. P. Freyssinier, "White lighting," Color Res. Appl. **38**, 82-92 (2013).
33. Y. Ohno and M. Fein, "Vision experiment on white light chromaticity for lighting," in *CIE/USA-CNC/CIE Biennial Joint Meeting,* (Davis, USA, 2013).
34. H. Akaike, "A new look at the statistical model identification," IEEE Transactions on Automatic Control **19**, 716-723 (1974).
35. V. Ekroll and F. Faul, "A simple model describes large individual differences in simultaneous colour contrast," Vision Res. **49**, 2261-2272 (2009).
36. B. Pearce, S. Crichton, M. Mackiewicz, G. D. Finlayson, and A. Hurlbert, "Chromatic illumination discrimination ability reveals that human colour constancy is optimised for blue daylight illuminations," PLoS ONE **9**, e87989 (2014).
37. L. Arend and A. Reeves, "Simultaneous color contancy," J. Opt. Soc. Am. A **3**, 1743-1751 (1986).
38. K. J. Linnell and D. H. Foster, "Scene articulation: dependence of illuminant estimates on number of surfaces," Perception **31**, 151-159 (2002).
39. D. H. Foster and S. M. C. Nascimento, "Relational color constancy from invariant cone-excitation ratios," Proceedings of the Royal Society of London Series B-Biological Sciences **257**, 115-121 (1994).
40. H. E. Smithson, "Sensory, computational and cognitive components of human colour constancy," Philosophical Transactions of the Royal Society B-Biological Sciences **360**, 1329-1346 (2005).
41. V. Ekroll and F. Faul, "New laws of simultaneous contrast?," Seeing and Perceiving **25**, 107-141 (2012).
42. J. M. Bosten and J. D. Mollon, "Kirschmann's fourth law," Vision Res. **53**, 40-46 (2012).
43. V. Ekroll, F. Faul, and G. Wendt, "The strengths of simultaneous colour contrast and the gamut expansion effect correlate across observers: Evidence for a common mechanism," Vision Res. **51**, 311-322 (2011).

Optics EXPRESS

## 1. Introduction

Chromatic adaptation, the ability of the visual system to (partially) adapt to changes in the color of the illumination, is an important aspect to consider when predicting the color appearance of a stimulus under varying viewing conditions. Indeed, chromatic adaptation transforms (CAT), models that predict the adaptive shift due to chromatic changes in lighting/viewing conditions, are an integral part of color appearance models (CAMs). Today, one of the most widely used CATs is the CAT02 transform [1] embedded in CIECAM02 [2]. This CAT, like many others, has been developed based on one or more sets of corresponding colors (CC), which are stimuli that appear equal in color under different illumination conditions. However, for most existing CC sets, the adaptive conditions were limited to (near) neutral illuminants [1], while new solid-state lighting technologies open up a range of potentially high chroma, colored illuminants for which the applicability of existing CAT can be questioned as the degree of adaptation tends to decrease as the adaptive field become more chromatic [3, 4]. For more information on chromatic adaptation, its link with physiology and its models and on the derivation of corresponding colors the reader is referred to part I of this study [5].

In this paper, the 12 corresponding memory color sets obtained in part I using a novel memory color matching method are extended to a set of 156 sets by including memory matches under 9 additional, more colored illuminants. The adapting luminance is the same as before, 760 cd/m² (approximately 2600 lux). Each sets contains corresponding colors for five familiar objects. After an analysis of the experimental results, the new corresponding color data set was used to test the performance of various chromatic adaptation transform models from literature. Finally, a model for the effective degree of adaptation obtained under the thirteen illumination conditions was also developed.

## 2. Methods

### *2.1 Experiments*

#### 4.1.1 Experimental setup

Memory colors were obtained under a total of 13 different adapting illuminants for five objects: a gray cube, a green apple, a ripe lemon, a ripe tomato and a blue smurf. Objects were selected to sample different parts of the hue circle. Although gray is not really a memory color, it is also an internal reference 'color' that has often been used in color constancy research. In this paper, 'gray' is therefore grouped together with actual memory colors for brevity. Illumination conditions were chosen to represent a typical light source chromaticity on or near the blackbody and daylight loci, as well as more colored chromaticities: a neutral [N] obtained by Smet et al. [6, 7], EEW, D65, illuminant A [A], Planckian radiators of 2000K [P2k], 4000K [P4k], 12000K [P12k] and infinite K [PInf]; and five high chroma sources (Red [R], Yellow [Y], Green [G], Blue [B] and Magenta [M]). Data and results on the neutral illuminants [N], EEW, D65 and [P4k] has been reported in part I of this study [5]. The chromaticity of the all 13 illuminants in the CIE 1976 *u'v'* diagram for the CIE 1964 observer has been plotted in Fig. 1.

As this study focusses on exploring the feasibility of the memory color matching method and especially on the impact of illuminant color on (the degree of) chromatic adaptation, the adaptive field luminance of the spectrally neutral background was limited to a single value, approximately 760 cd/m² (~2600 lux). As also described in part I the background scene, illustrated in Fig. 2(a), had a field of view of approximately 50° and was populated with various spectrally neutral (gray) 3D objects to enhance scene realism and to provide depth, parity and illumination cues, which have been reported to increase color constancy and chromatic adaptation [8]. Colored objects were not included to avoid biasing the overall

Optics EXPRESS

background chromaticity [9] compared to the *gray world*. In color constancy research, the latter is often assumed as a possible cue to illuminant estimation.

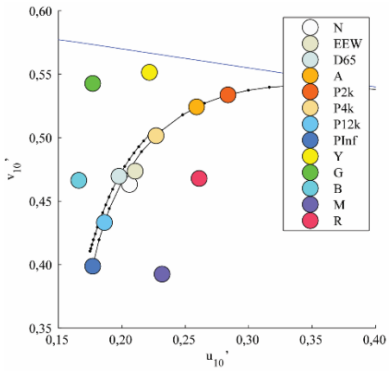


Fig. 1. CIE 1976 *u'v'* chromaticity of the thirteen illumination conditions.

The background was illuminated by a calibrated data projector that allowed for the independent adjustment of stimulus area and background area. This setup essentially separates the adaptive shift from the illuminant colorimetric shift present in asymmetric matching data obtained using reflective samples. The color of the background illumination and the color of test objects of various shapes and sizes could be easily independently controlled by the use of a small mirror underneath the test object, a careful relative positioning of the projector, background and observer, and by the projection of a simple two-color image. A side view of the experimental setup is schematically presented in Fig. 2(b).

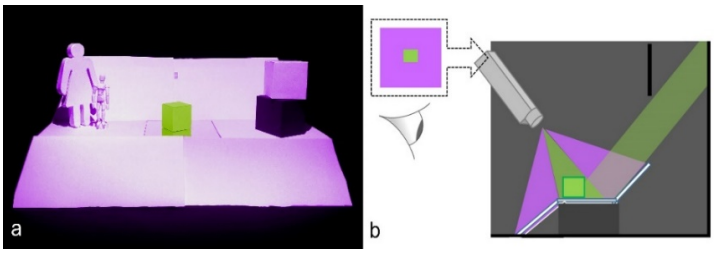


Fig. 2. (a) Illustration of the background scene under magenta illumination with the cube in a green starting chromaticity (see experimental procedure). (b) Side view schematic of the experimental setup.

During the experiments, observers could adjust the CIE *u'v'* chromaticity and luminance of the test object by using the arrow keys on a keyboard. Each memory color setting was spectrally recorded using a telespectroradiometer (Bentham TEL301 telescope coupled to an Ocean Optics QE65 Pro spectrometer). Chromaticity coordinates and luminance values have been calculated from the spectral radiance measurements using the CIE 1964 (10°) observer.

### 4.1.2 Experimental procedure

The experimental procedure is identical to that reported in part I of this study [5], as the memory color matches for the 9 colored illuminants were obtained in the same experiments as the 4 neutral ones reported earlier. Basically, an observer was required to make 4 memory color matches – each with a different starting chromaticity to avoid starting bias – for each object and illumination condition. Matches were collected in two session on separate days to avoid fatigue, whereby the presentation order of the illumination conditions was randomized to minimize order bias. To ensure a representative degree of adaptation to each new illuminant, observers were requested to wait for approximately 15 seconds before starting to make his/her memory color match. It is known that 50% of the steady-state adaptation level

Optics EXPRESS

is reached within the first few seconds [10]. By the time an observer has finished his match, which takes at least one minute, approximately 90% or more of the steady-state adaptation level will have been reached. To minimize the potential for a mixed adaptation state between the familiar object color and the color of the background adapting field and maximize adaptation to the latter observers were also instructed not to stare at the presented familiar object while making their matches. After each satisfactory match, the observer was asked to rate the quality of the match on a 0-10 scale. The match was then spectrally recorded and the illumination was changed to a new condition.

#### 4.1.3 Observers

Twenty-three color-normal observers, as tested by the Ishihara-24-plate test, participated in the experiments. The average age of the observers was 33 years with a standard deviation of 10 years. For each object and illumination condition, memory colors were determined by ten observers (5 male and 5 female). A prerequisite for each observer was familiarity with the prototypical color of the object presented.

### *2.2 Analysis*

#### 4.2.1 Observer variability and average observer uncertainty

As in part I [5], inter-observer memory color variability was estimated by calculating for each individual observer for each illuminant condition and object the *u'v'* color difference, $DE_{u'v'}$, with the mean memory color of all observers and taking the median (MedCDM, Median color difference with the mean). Because of the skewed distribution of color differences values due to the lower bound at zero, a median instead of a mean was selected. Intra-observer variability was evaluated with regard to an observer's own mean memory color (of the four matches per illumination condition per object). Additionally, observer variability was also assessed using STRESS, the Standardized-Residual-Sum-of-Squares [11]. Low values signify good agreement, either within (intra) or between (inter) observers.

The uncertainty (in *u'v'* units) of the average observer's memory color of an object for each illluminant was estimated as the average length of the minor and major axes of the standard error ellipses around the mean memory color.

Finally, the reliability of the concept of an *average observer* based on a limited number of individual observers was assessed by an *ICC(2,n)* Intraclass Correlation Coefficient [12]. The *ICC* ranges from 0 (no agreement) to 1 (perfect agreement).

#### 4.2.2 Derivation of Corresponding Colors (CC)

Corresponding colors are stimuli that have the same color appearance under different illumination (adaptive) conditions. In this study the target colors for matching under each illumination condition were the same (i.e. the object memory colors), therefore, 156 *(=13(13-1))* sets of corresponding color pairs could be derived by a pair wise combination of the memory color data (i.e. the chromaticity values calculated from the measured spectral data) obtained for each illuminant. For example, A to D65, D65 to A, A to EEW, etc.

#### 4.2.3 Testing Chromatic Adaptation Transforms (CAT)

The predictive performance of various linear and nonlinear CATs was tested using the new corresponding color data sets. Linear CATs included a one-step (Eq. (10), Part I: [5]) and a two-step (Eq. (12), Part I: [5]) von Kries CAT with cone sensors determined using the HPE [13], CAT02 [2], SHARP [14], BFD[15], CMC [16], BS & BS-PC [17] primaries. Regular *XYZ* primaries and the CAT adopted in RLAB [13] were also included. *XYZ* were included as primaries because CIELAB performs, what is called a 'wrong', von Kries chromatic adaptation on the *XYZ* tristimulus values themselves. Nonlinear CATs included the one adopted in the Hunt model [18] and the one developed by Nayatani [19].

Optics EXPRESS

Model performance was investigated by setting the degree of adaptation (or discounting the illuminant) $D$ to 1 (full adaptation or full discounting-the-illuminant), by calculating it according to three functions ($D_{CAT02}$ [2], $D_{CMCCAT97}$ [20] and $D_{CMCCAT2000}$ [16]) published in literature that take the adapting luminance and surround brightness ('*average*', '*dim*' or '*dark*') into account and by optimizing the value of $D$ such that the median CIE 1976 $DE_{u'v'}$ was minimized for each corresponding color set. Note that the Hunt and Nayatani models do not include discounting-the-illuminant factors. However, analogous to RLAB, the Hunt model was extended with a $D$ factor to adjust the contribution of the chromatic adaptation factors $F_{\rho\gamma\beta}$. The Hunt model also includes a correction for the Helson-Judd effect whereby achromatic surfaces lighter and darker than the background respectively take on the hue and complementary hue of the illumination. Although likely of little importance in practical viewing conditions [13], the impact of its effect was examined by adding a "*degree of Helson-Judd correction*" $D_{HJ}$ to the model. $D_{HJ}$ was optimized to minimize $DE_{u'v'}$ or set to either 0 (no HJ correction) or 1 (full HJ correction). Because the Nayatani model is less easily extended with a degree of discounting-the-illuminant it was kept as is.

In total, 14 (sub)models x 8 sensor matrices (= 112) were tested using the 156 corresponding memory colors data sets. For comparison, model performance was also determined using 8 corresponding color sets (26 subsets in total, see also details in Table 1 in Appendix A) published in literature: CSAJ [21], Helson [22], Lam & Rigg [15], LUTCHI [23], Kuo & Luo [24], Breneman [25], Braun & Fairchild [26] and McCann [27]. Performance was evaluated as the median color differences between the predicted and experimental corresponding colors. The following color difference formulas were used: $DE_{u'v'}$ (CIE 1976 *u'v'* chromaticity diagram), $DE^*_{ab}$ (CIELAB) and $DE00$ (CIEDE2000) [28].

## 3. Results and discussion

### 5.1 Observer variability

The median intra- and inter-observer MedCDM values calculated across all objects and illumination conditions are respectively *0.0133* and *0.0155 u'v'* units. Average observer standard uncertainty is *0.0075 u'v'* units and STRESS values are respectively *40%* and *41%*. The STRESS value for intra-observer variability is much higher than the *22%* reported in [29] for memory color ratings under D65, indicating that observers found matching less easy than rating or that there is potentially a starting bias for the individual matches., The value for the inter-observer variability, on the other hand, was only slightly worse than the reported value of *36%*, indicating that averaging the individual matches results in a similar level of agreement as in a memory color rating experiment. In addition, it also indicates that any potential starting bias is largely reduced or even completely eliminated in the averaged results. As expected, compared to color discrimination studies where the reference color is the same for each observer, the inter-observer variability for the memory color matching in the present study is larger, but only slightly: e.g. STRESS values of 35% [30] or 37% [31] compared to the 41% found for this study. The good to excellent observer agreement—note that individual observer memory colors need not be identical—was also confirmed by the high value of the *ICC(2,n)* intraclass correlation coefficient (*0.86*).

### 5.2 Testing Chromatic Adaptation Transforms (CAT)

The prediction errors in terms of $DE_{u'v'}$, $DE^*_{ab}$ and *DE00* for the various models (using their native sensor spaces; HPE for the von Kries transforms) for the corresponding memory color data sets are given in Table 2. The prediction errors for the 26 sets from literature are gathered in Table 3. For comparison, the prediction errors for both corresponding color data sets are also given for the von Kries models with the widely used CAT02 sensor space in Table 4 in Appendix B. The data sets are divided in subsets according to the chromaticity of

Optics EXPRESS

their illumination conditions: '*all*', '*neutral to neutral*' (cfr. part I: [5]), '*non-neutral to non-neutral*', *'neutral to non-neutral*' and '*non-neutral to neutra*l'. The chromaticity regions of (non) neutrality—see Table 2—were chosen based on literature [6, 7, 32, 33].

**Table 2. Prediction error in terms of $DE_{u'v'}$, $DE^*_{ab}$ and DE*00* for the various tested models (with their native sensors) for the entire corresponding memory color data sets and several subsets.**

| Model #: | 1 | 2 | 3 | 4 | 5 | 6 | 7 | 8 | 9 | 10 | 11 | 12 | 13 | 14 |
|---|---|---|---|---|---|---|---|---|---|---|---|---|---|---|
| Model description: | von Kries, $D_{1,2}$ = opt. (2-step: A to EEW to B) | von Kries, $D_1$ = opt. (1-step: A to B) | von Kries $D_{1,2}$ = 1 (2:step: A to EEW to B) | von Kries, $D_{1,2} = D_{CAT02}$ (2-step: A to EEW to B), | von Kries, $D_{1,2} = D_{cmccat2000}$ (2-step: A to EEW to B) | von Kries, $D_{1,2} = D_{cmccat97}$ (2-step: A to EEW to B) | RLAB model, $D_{1,2}$ = opt. | RLAB model, no *D* | Hunt model, $D_{1,2}$ = opt., $D_{HJ}$ = opt. | Hunt model, no *D*, $D_{HJ}$ = *opt.* | Hunt model, $D_{1,2}$ = *opt.*, no *HJ* | Hunt model, $D_{1,2}$ = *opt.*, full *HJ* | Hunt model, no *D*, *no HJ* | Nayatani model, no *D* |
| | ***All corresponding color data sets*** | | | | | | | | | | | | | |
| **DE*u'v'*(1e-3)** | 4.7 | 6.0 | 39.4 | 26.9 | 39.4 | 26.9 | 32.2 | 33.7 | 32.2 | 32.0 | 32.0 | 44.3 | 32.0 | 47.1 |
| **DE*ab** | 4.0 | 5.0 | 27.9 | 21.0 | 27.9 | 21.0 | 21.9 | 23.7 | 21.6 | 21.3 | 21.3 | 29.5 | 21.3 | 36.4 |
| **DE*00*** | 2.2 | 2.6 | 11.2 | 8.3 | 11.2 | 8.3 | 9.7 | 9.9 | 9.4 | 9.4 | 9.4 | 12.4 | 9.3 | 14.2 |
| | ***Neutral to neutral only*** ***(CCT ≥ 3500 && CCT ≤ 10000 && \|Duv\| ≤ 0.015 for both illuminations conditions)*** | | | | | | | | | | | | | |
| **DE*u'v'*(1e-3)** | 1.6 | 2.0 | 10.3 | 6.5 | 10.3 | 6.5 | 7.5 | 8.5 | 7.9 | 7.9 | 7.9 | 11.6 | 7.9 | 12.4 |
| **DE*ab** | 1.6 | 1.9 | 6.1 | 3.7 | 6.1 | 3.7 | 4.2 | 4.9 | 4.5 | 4.6 | 4.5 | 6.9 | 4.5 | 8.1 |
| **DE*00*** | 0.9 | 1.0 | 3.3 | 2.1 | 3.3 | 2.1 | 2.5 | 2.8 | 2.8 | 2.8 | 2.8 | 3.7 | 2.8 | 4.1 |
| | ***Non-neutral to non-neutral*** ***(CCT < 3500 && CCT > 10000 && \|Duv\| > 0.015 for both illuminations conditions)*** | | | | | | | | | | | | | |
| **DE*u'v'*(1e-3)** | 4.9 | 6.2 | 42.0 | 27.7 | 42.0 | 27.7 | 33.3 | 35.9 | 32.8 | 32.8 | 32.8 | 46.1 | 32.8 | 48.6 |
| **DE*ab** | 4.2 | 5.4 | 28.8 | 21.7 | 28.8 | 21.7 | 23.2 | 25.4 | 22.7 | 22.6 | 22.8 | 31.6 | 22.4 | 37.4 |
| **DE*00*** | 2.2 | 2.7 | 11.6 | 8.5 | 11.6 | 8.5 | 10.0 | 10.5 | 9.6 | 9.7 | 9.6 | 12.7 | 9.6 | 14.7 |
| | ***Neutral to non-neutral*** | | | | | | | | | | | | | |
| **DE*u'v'*(1e-3)** | 4.5 | 5.2 | 34.7 | 22.2 | 34.7 | 22.2 | 29.3 | 29.5 | 28.3 | 28.3 | 28.5 | 38.1 | 28.8 | 42.4 |
| **DE*ab** | 3.8 | 4.3 | 25.4 | 16.6 | 25.4 | 16.6 | 20.9 | 20.9 | 18.8 | 18.8 | 18.8 | 27.9 | 19.2 | 33.1 |
| **DE*00*** | 2.0 | 2.0 | 10.2 | 7.3 | 10.2 | 7.3 | 8.7 | 8.7 | 7.8 | 7.8 | 7.8 | 10.8 | 8.0 | 13.4 |
| | ***Non-neutral to neutral*** | | | | | | | | | | | | | |
| **DE*u'v'*(1e-3)** | 4.2 | 5.4 | 38.1 | 26.2 | 38.1 | 26.2 | 29.7 | 32.5 | 31.4 | 31.4 | 31.4 | 42.1 | 31.4 | 43.5 |
| **DE*ab** | 3.8 | 4.3 | 23.5 | 15.4 | 23.5 | 15.4 | 18.1 | 20.4 | 19.9 | 19.0 | 19.0 | 25.7 | 19.0 | 31.2 |
| **DE*00*** | 1.8 | 2.4 | 11.1 | 8.2 | 11.1 | 8.2 | 8.7 | 9.7 | 9.4 | 9.4 | 9.4 | 12.3 | 9.4 | 13.4 |

Comparing the values for the various models in Table 2 it is clear that a simple von Kries CAT with optimized *D* values and applying a two-step transform performs the best for all investigated subsets. The results also show that a one-step von Kries CAT performed directly between illumination conditions *A* and *B* performs slightly, but significantly (Wilcoxon signed rank tests (WSR), $p < 0.05$), worse. Both models also have predictive errors that are substantially smaller than the standard uncertainty on the average observer. Also note that these are the only two models whereby the degree of effective adaption is free to range between *completely no adaptation* and *completely full adaptation*.

In the other models, *D* is either completely lacking (e.g. the Nayatani model), is acting on some other function regulating adaptation (e.g. in the RLAB and Hunt models), is completely determined by the adapting luminance and surround viewing conditions ($D_{CAT02}$, $D_{CMCCAT97}$ and $D_{CMCCAT2000}$) or is kept fixed. Obviously the reduced freedom in these models could have a negative impact on their predictive performance. The Akaike Information Criterion (AIC) [34] was therefore used to compare the performance of the models while taking the degrees of freedom available during the optimization into account. The analysis showed that the two-step model has the better performance compared to the one-step CAT and all other models. The results of the model is therefore a good benchmark for the performance that should be achievable under the von Kries assumption. Any remaining

Optics EXPRESS

model predictive errors with corresponding color data are then either due to additional effects, such as for example simultaneous contrast, subtractive mechanisms and nonlinearities not included in the model, or are the result of noise in the data set itself.

A first restrictive model is the von Kries CAT with $D$ set to 1. From Table 2, it is clear that there are large prediction errors, especially for sets involving non-neutral illumination conditions. Models that include a $D$-function based on the adapting luminance similarly result in large prediction errors: the largest errors occur for $D_{CMCCAT2000}$ as $D = 1$ for the adapting luminance (760 cd/m²) and dark surround of this study; for both $D_{CAT02}$ and $D_{CMCCAT97}$ $D = 0.8$. Although RLAB does better than the von Kries CATs with $D = 1$, it provides a worse prediction than the von Kries CATs which use $D_{CAT02}$ and $D_{CMCCAT97}$. Despite RLAB's correction for the chromaticity of the illumination (see Eq. (7), Part I [5]), prediction errors are still very large, probably due to the relatively small contribution of the chromaticity compared to that of the high adapting luminance in this study. For neutral illumination conditions RLAB has a much better predictive performance, one that is comparable to the uncertainty on the average observer. The Hunt and Nayatani nonlinear models perform poorly for sets including non-neutral illumination conditions. This is surprising given their very complex structure that tries to include many of the mechanisms involved in human color vision. Part of the poor performance could, at least for the Nayatani model, be attributed to the lack of any discounting of the illuminant (no $D$ factor that could be optimized). However, even then it has a substantially higher prediction error than other CATs where $D$ has been kept fixed (e.g. von Kries with $D = 1$, RLAB without $D$ contribution and the Hunt model without $D$ or $D_{HJ}$). The Hunt model on the other hand, does include such a factor. However, the contribution of chromaticity to the chromatic adaptation factors has the same functional form as the one in RLAB. Therefore, here also, the effective degree of adaptation might be mainly driven by the high adapting luminance. The results further show that the Helson-Judd effect included in the Hunt model has little impact on predictive performance.

For subsets composed of neutral adaptive conditions both nonlinear models reach performance levels comparable to other corresponding color data sets published in literature (see Table 3). Similar results were obtained for the other models as well. Especially the von Kries CATs with free effective adaptation level (models 1 and 2) had substantially lower predictive errors for the neutral corresponding memory color sets than for the neutral sets from literature.

From Table 3, it can be observed that the Hunt models and RLAB model with optimized $D$ performed very well for the literature sets. For each subset they were among the best, together with the one- and two-step von Kries models with free effective adaptation level. Of the latter two, the two-step von Kries model was again the better model (WSR, $p < 0.05$), except for the '*all*' data set when estimating model performance using $DE_{u'v'}$. Also, in qualitative agreement with the results for the corresponding memory color data sets, the predictive errors for sets containing non-neutral illumination conditions still tend to be larger than for ones with neutral adaptive conditions, although not as severe. This indicates a systematic failure of the models to fully account for the chromaticity of the illumination, either through an appropriate function predicting the degree of chromatic adaptation or discounting-the-illuminant or through some other means, such as for example inclusion of a simultaneous color contrast model. It is also possible that observers find it more difficult to make or select an appropriate match under non-neutral conditions. Ekroll [35] has shown that *saturation scale truncation and extension*, which is caused by simultaneous contrast and crispening, can lead to increased observer variability in asymmetric matching experiments. Apparently, stimuli of the same hue as the background cannot appear less saturated than the background itself. Therefore, an observer might have problems when trying to produce, for example, a match on a violet background of a violet stimulus presented on a white background, as on the white background less saturated violets are possible. Presented with

Optics EXPRESS

such a difficulty an observer might either choose to make a saturation match in the opponent hue or he/she might make a hue match in which case he cannot match saturation. In either case a perfect match is impossible and the different observer strategies will further increase observer variability.

**Table 3. Prediction error in terms of $DE_{u'v'}$, $DE^*_{ab}$ and $DE00$ for the various tested models (with their native sensors) for the 26 corresponding color data sets published in literature.**

| Model #: | 1 | 2 | 3 | 4 | 5 | 6 | 7 | 8 | 9 | 10 | 11 | 12 | 13 | 14 |
|---|---|---|---|---|---|---|---|---|---|---|---|---|---|---|
| Model description: | von Kries, $D_{1,2}$ = opt. (2-step: A to EEW to B) | von Kries, $D_1$ = opt. (1-step: A to B) | von Kries $D_{1,2}$ = 1 (2:step: A to EEW to B) | von Kries, $D_{1,2} = D_{CAT02}$ (2-step: A to EEW to B), | von Kries, $D_{1,2} = D_{cmccat2000}$ (2-step: A to EEW to B) | von Kries, $D_{1,2} = D_{ccmccat97}$ (2-step: A to EEW to B) | RLAB model, $D_{1,2}$ = opt. | RLAB model, no *D* | Hunt model, $D_{1,2}$ = opt., $D_{HJ}$ = opt. | Hunt model, no *D*, $D_{HJ}$ = *opt.* | Hunt model, $D_{1,2}$ = *opt.*, no *HJ* | Hunt model, $D_{1,2}$ = *opt.*, full *HJ* | Hunt model, no *D, no HJ* | Nayatani model, no *D* |
| ***All corresponding color data sets*** | | | | | | | | | | | | | | |
| **DE*u'v'*(1e-3)** | 7.8 | 7.5 | 12.0 | 10.2 | 11.7 | 10.1 | 7.7 | 10.4 | 7.2 | 13.5 | 7.3 | 7.6 | 14.2 | 13.1 |
| **DE*ab** | 5.1 | 5.2 | 7.0 | 6.2 | 6.7 | 6.4 | 5.0 | 6.6 | 5.8 | 10.0 | 5.9 | 5.7 | 10.5 | 7.8 |
| **DE*00*** | 3.1 | 3.3 | 3.9 | 3.2 | 3.7 | 3.3 | 3.2 | 3.7 | 3.4 | 5.8 | 3.5 | 3.4 | 6.0 | 4.3 |
| ***Neutral to neutral only (CCT ≥ 3500 && CCT ≤ 10000 && \|Duv\| ≤ 0.015 for both illuminations conditions)*** | | | | | | | | | | | | | | |
| **DE*u'v'*(1e-3)** | 6.4 | 6.5 | 9.9 | 7.9 | 9.6 | 8.8 | 6.7 | 7.2 | 5.8 | 8.5 | 5.8 | 5.8 | 9.2 | 10.6 |
| **DE*ab** | 4.3 | 4.4 | 5.2 | 4.6 | 5.1 | 4.7 | 4.5 | 4.4 | 4.9 | 7.0 | 5.0 | 4.9 | 7.3 | 5.9 |
| **DE*00*** | 2.6 | 2.7 | 2.8 | 2.7 | 2.8 | 2.8 | 2.7 | 3.1 | 2.8 | 4.3 | 2.8 | 3.0 | 4.5 | 3.7 |
| ***Non-neutral to non-neutral (CCT < 3500 && CCT > 10000 && \|Duv\| > 0.015 for both illuminations conditions)*** | | | | | | | | | | | | | | |
| **DE*u'v'*(1e-3)** | 8.2 | 8.3 | 14.6 | 11.6 | 14.4 | 11.3 | 7.8 | 10.7 | 7.7 | 16.1 | 7.8 | 7.8 | 17.4 | 14.8 |
| **DE*ab** | 5.7 | 5.8 | 8.1 | 7.1 | 8.0 | 7.0 | 5.3 | 7.4 | 6.1 | 10.9 | 6.2 | 6.2 | 11.5 | 8.3 |
| **DE*00*** | 3.6 | 3.7 | 4.7 | 3.8 | 4.5 | 3.8 | 3.6 | 4.6 | 3.7 | 6.1 | 3.7 | 3.7 | 6.3 | 4.8 |
| ***Neutral to non-neutral*** | | | | | | | | | | | | | | |
| **DE*u'v'*(1e-3)** | 6.3 | 6.5 | 11.3 | 8.5 | 10.6 | 8.6 | 6.4 | 8.3 | 6.5 | 16.7 | 6.5 | 6.4 | 17.7 | 11.9 |
| **DE*ab** | 4.4 | 4.8 | 5.7 | 4.9 | 5.7 | 4.9 | 4.6 | 5.5 | 4.4 | 10.7 | 4.4 | 4.3 | 11.3 | 7.3 |
| **DE*00*** | 2.7 | 2.8 | 3.1 | 2.7 | 2.9 | 2.8 | 2.7 | 3.2 | 2.7 | 4.9 | 2.7 | 2.7 | 5.1 | 3.7 |
| ***Non-neutral to neutral*** | | | | | | | | | | | | | | |
| **DE*u'v'*(1e-3)** | 9.5 | 9.9 | 12.9 | 10.5 | 12.1 | 10.9 | 8.0 | 13.0 | 8.3 | 20.5 | 8.6 | 8.3 | 22.0 | 13.7 |
| **DE*ab** | 4.9 | 5.2 | 7.9 | 6.5 | 6.8 | 6.8 | 5.0 | 7.3 | 5.0 | 11.5 | 5.9 | 5.1 | 12.1 | 7.7 |
| **DE*00*** | 3.6 | 3.6 | 4.9 | 3.7 | 4.3 | 3.8 | 3.6 | 4.8 | 3.7 | 6.9 | 3.7 | 3.8 | 7.3 | 4.9 |

Up till now, model performance has been investigated using each model's built-in (native) sensor matrices. The impact of the choice of sensor primaries on model error prediction has also been determined for 7 other sets of primaries. The $DE_{u'v'}$, $DE^*_{ab}$ and *DE00* prediction errors for each have been plotted in Fig. 3. The left graphs are the errors for the memory color sets, the right those for the literature sets.

It is clear from Fig. 3 that in general the biggest impact on the prediction error is due to the model type and not the choice of sensor primaries, except for the XYZ primaries. These perform, as expected, very poorly compared to the other primaries, indicating that CIELAB's built-in CAT, often referred to as wrong von Kries, is indeed "wrong" and results in substantial errors. For most models, changing the sensor primary set does not result in substantial changes in $DE_{u'v'}$, especially for the von Kries models with free effective adaptation state (models *1* & *2*) and the Nayatani model. For most of the Hunt (sub)models the best primaries are the Bradford BFD (≈ 0.028 $DE_{u'v'}$ units). The best sensor spaces for the von Kries models with optimized *D* are the Bradford BDF matrix (model 1 & 2: $DE_{u'v'}$ *0.0038 units*) and CMC (model 1: *0.0072* $DE_{u'v'}$ *units*) & HPE matrix (model 2: *0.0075* $DE_{u'v'}$ *units*) for the memory color data sets and the sets from literature respectively. The reason that the currently best CIE CAT, i.e. CAT02, was not the 'best' among these models

Optics EXPRESS

is three-fold: first, CAT02 was optimized for only a limited subset of the 26 corresponding color data sets from literature; second, the current analysis uses a median instead of mean or root-mean-square to provide a more reliable estimate for central tendency and finally, the *D* optimization was performed by using $DE_{u'v'}$ as to not bias the results by the intrinsic chromatic adaptation transform present in CIELAB when calculating $DE^*_{ab}$ or *DE00*.

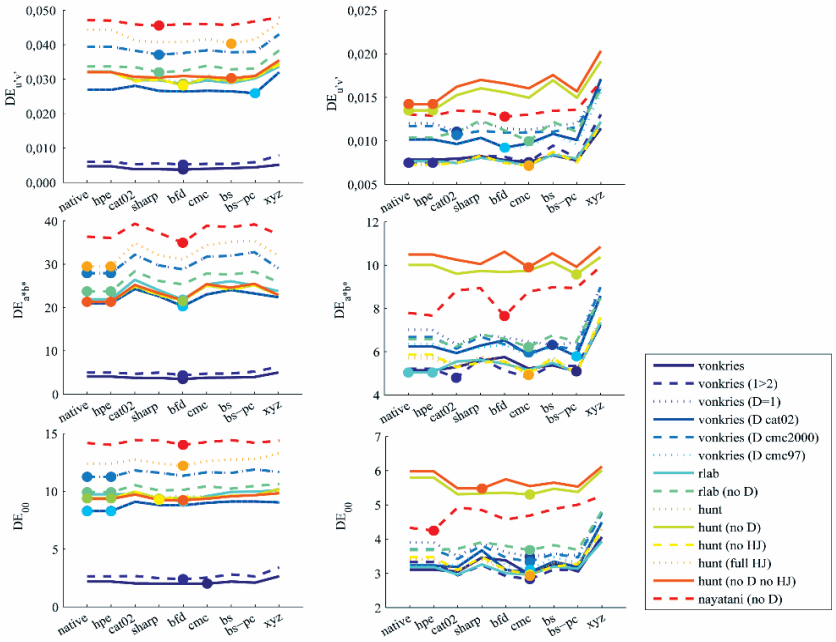


Fig. 3. Prediction errors as a function of various sensor primary sets for each of the models investigated. Dots represent the minimum error prediction – sensor space combination for each of the models. Left: Results for the corresponding memory color sets. Right: Results for the sets from literature.

Using $DE^*_{ab}$ for the analysis BFD is again the best sensor space for von Kries models 1 & 2 and most other models for the memory color sets, while for the data sets from literature the CAT02 matrix is found as the best for the one-step von Kries model (model 2: 4.8 $DE^*_{ab}$ units) and BS-PC for the two-step model (model 1: 5.1 $DE^*_{ab}$ units). RLAB performs optimally for the HPE sensor space (5.0 $DE^*_{ab}$ units). The Nayatani and most of the Hunt models have optimal performance for the BFD for the memory color sets, while optimal performance for several of the Hunt models shifted to the CMC sensor space for the literature data set.

An analysis based on *DE00* lead again to switches in optimal sensor space for several models. In this case, for the one-step and two-steps von Kries models BFD (model 1: 2.4 *DE00* units) and CMC (model 2: 2.0 *DE00* units) are respectively the best sensor matrices for the corresponding memory color sets. For the literature sets, the CMC matrix is the best for all models, except for one of the Hunt (no D, no HJ) and the Nayatani models which have the best performance for respectively the SHARP and HPE matrices. Assuming *DE00* is indeed the best measure (although note the potential bias due to the built-in "wrong" von Kries chromatic adaptation transform) to assess these median corresponding color differences the following rank order can be observed: the CMC sensor space is best (note that this set was indeed derived by Li et al. [16] by optimization to all 26 literature sets), closely followed by the BFD and the CAT02 matrices. Although, the HPE matrix, which more closely resembles actual cone responsivities, would also result in adequate performance for physiologically inspired model development based on the two-step von Kries (<0.2 *DE00* units difference with optimal CMC performance). For other models, the

Optics EXPRESS

difference can be larger and the ranking of the CMC and HPE can be switched in some cases.

Finally, given the relatively small differences in performance between most sensor spaces for a given *DE*-measure and the fact that because of these small differences the 'best' sensor space is highly dependent on the measure used to assess its performance, most of these sensor spaces can be used interchangeably without resulting in substantial errors.

## 4. Modelling the effective degree of adaptation and the von Kries law

From the above analysis it is clear that a failure to accurately account for the effective degree of adaptation can lead to substantial decreases in predictive performance. Such failure could be due to either incompleteness (e.g. no chromaticity dependence) or plain error in the model itself, to noise in the psychophysical data; or to other (additional) processes contributing to object color appearance, such as for example simultaneous contrast.

Given that the corresponding color data, and especially the memory color based data, could be adequately predicted by a simple von Kries chromatic adaptation transform it is reasonable to assume that (independent) gain control of the sensors is the main mechanism determining object color appearance under different illumination conditions in a neutral surround. However, because a von Kries CAT with the effective degree of adaptation *D* set to *1* performed sub-optimally it is desirable to have a model for the effective degree of adaptation. Although such models have been developed, for example the $D_{CAT02}$ or RLAB's $p_x$, their performance was worse compared to the performance of a von Kries CAT with optimized *D*.

A model for the optimized *D* for the memory color data sets was therefore derived and the predictions errors of a two-step von Kries CAT with HPE sensor primaries that incorporates the modelled degree of adaptation were compared to the those obtained with the optimized *D* values themselves. Several basic color spaces were explored to find a good fit to the optimized D values using a simple model. A bivariate Gaussian fitted to the data in a log compressed Macleod-Boyton like chromaticity diagram using the HPE primaries was found to work very well ($R^2$ = 0.87, *STRESS* = 13%). A plot of the median optimized *D* values for the 13 illumination conditions and the fitted bivariate Gaussian model has been plotted in Fig. 4 in the CIE *u'v'* chromaticity diagram.

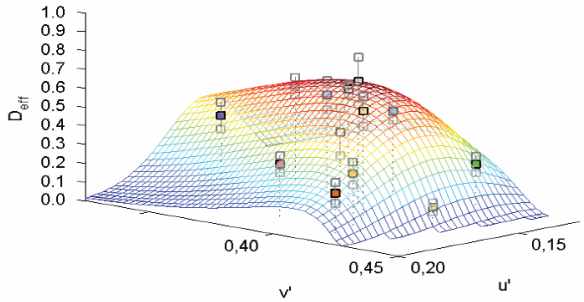


Fig. 4. Median optimized degrees of adaptation for the thirteen illumination conditions in the memory color experiments (colored square data points) and the modelled degree of effective adaptation (mesh). The error bars of the optimized *D* values are also plotted.

It is clear that the model approximates the optimized *D* values quite well, which was confirmed by the low median prediction error for the corresponding memory color data sets ($DE_{u'v'} = 0.0088$, $DE^*_{ab} = 5.3$ and $DE00 = 2.8$). From Fig. 4 it is also clear that overall the median degree of effective adaptation $D_{eff}$ decreases as the illumination becomes more chromatic, but with a clear dependency on chromatic direction. $D_{eff}$ is higher for neutral to bluish illuminations than for yellowish, reddish or greenish ones and falls off less rapidly

Optics EXPRESS

along the daylight locus. Heightened color constancy (i.e. effective adaptation) for bluish illuminants was also found by Pearce et al. [36] by using a color discrimination technique. They attributed their results to the human visual system being optimized for bluish illuminations as these are more prevalent in daylight illuminations than yellowish, reddish and greenish ones.

From Fig. 4 it is also clear that the overall degree of effective adaptation is quite low, even for the neutral adaptive conditions ($D \approx 0.67$) despite the very high luminance of the background (*760* cd/m²). Based on Eq. (4) in Part I [5], one would expect full adaptation. Although adaptation is rarely complete and the median value for the neutral adaptive condition is in agreement with values reported in literature for color constancy under laboratory conditions [8] and for appearance matches (rather than surfaces matches) [37], the results suggest that the viewing conditions were probably still insufficiently representative of real-life situations where higher chromatic adaptation levels are typical. Despite the high luminance and large field of view (50°) of the background scene, as well as the care taken to provide the observer with various cues to the illumination to increase the effective degree of adaptation, it is likely that the observers experienced a mixed adaptation state due to the presence of the dark surround caused by eye and head movements during the course of the experiments. Correcting for the dark surround using the correction factor $F$ in Eq. (4), Part I [5], the effective degree of adaptation in a surround of average luminosity would have been *0.84*. Other possible causes for the lower than expected degree of adaptation are that the background scene contained only spectrally unselective, i.e. *"gray"* objects. It has been shown that color constancy tends to increase as the visual system has several colored surfaces available to estimate the illuminant from [38], for instance through the (near) invariance of cone-excitation ratios under typical illuminant changes [39] or other relational color constancy mechanisms [8, 40]. However, colored objects were not added to the background scene as to not bias the overall background chromaticity, which might be used to estimate the illuminant [9]. Future experiments will therefore involve a more immersive environment with additional cues to the illumination condition and additional levels of the adapting luminance and background luminance factors to extend the current model for the effective degree of adaptation.

Simultaneous color contrast might also have affected the results, either directly or indirectly through saturation scale truncation and extension. While simultaneous color contrast with a background is typically assumed to induce color shifts *complementary* to the hue of the background and independent of the color of the stimulus, Ekroll and Faul [41] have found supporting evidence for color induction along the background-stimulus direction away from the background color. In addition, according to Kirschmann's fourth law, the magnitude of the simultaneous contrast effect is generally considered to increase with the excitation purity of the background in asymmetric matching experiments, although some studies have found magnitude saturation and even magnitude decreases for highly chromatic backgrounds [42]. Ekroll et al. [43] reported crispening effects around the background color that reduce to zero as its saturation increases. Such nonlinear effects and interaction between the stimulus and the background would cause distortions from the simple von Kries gain regulation, and would therefore impact the prediction errors and hence possibly the optimized degrees of adaptation $D$. The prediction error did increase for the more chromatic illumination conditions, especially for the red, yellow and green colored illuminants close to the spectrum locus, signaling deviations from the von Kries law. Note that such deviations could also be due to non-uniformity (-linearity) in the DE color space at more chromatic locations. Therefore, as an additional test of the von Kries model, the error prediction analysis was performed separately for the single pairs of corresponding colors of each familiar object. The more restrictive one-step von Kries model (*#2*), the one that maps directly between two illumination conditions, was used because otherwise one would have two degrees of freedom in a two dimensional chromaticity diagram which would obviously

Optics EXPRESS

(when *D* could also take on values outside the *0-1* range) lead to extremely small errors when mapping a single pair of corresponding colors. However, even in the case of one-dimensional mapping, low prediction errors were found, resp. *0.0040, 0.0033, 0.0017, 0.0029* and *0.0035* $DE_{u'v'}$ units for the neutral, red, yellow, green and blue familiar objects. This indicates that the average observer indeed makes matchings consistent with independent gain control. However, whether the underlying mechanism is actually von Kries adaptation at the photoreceptor level or other, possibly subtractive, processes at the opponent level cannot be ascertained from the data with certainty. However, additional simultaneous contrast effects are likely occurring given the above discussion and the fact that the larger prediction error for the entire corresponding color sets of 5 hues (*0.0060* $DE_{u'v'}$ units, see Table 2) can be interpreted as due to incompatible requirements for the value of the optimized *D* for the different familiar objects (resp. *0.49, 0.29, 0.43, 0.34* and *0.15* for the neutral, red, yellow, green and blue familiar objects). Although this discrepancy could just be due to the memory colors of the *average observer* not being stable enough, the high *ICC* value suggested otherwise. It is therefore more likely that the required different values for *D* are a reflection of interactions between the stimuli and the backgrounds, probably due to simultaneous contrast effects, which will be the topic of a future follow-up paper. Finally, also note that the magnitudes of the prediction errors are comparable to what are considered just-noticeable-differences in the CIE *u'v'* chromaticity diagram, which supports the use of memory color based internal references in asymmetric matching experiments designed to study chromatic adaptation mechanisms.

## 5. Summary and conclusions

In this paper, the 12 corresponding memory color sets for neutral illuminants obtained in part I [5] were extended to 156 sets by including memory matches under 9 additional, more colored illuminants (adaptive luminance of 760 cd/m²). As in part I for the neutral illuminants, the memory color matching method was found to provide corresponding color data that complies well with the von Kries law, which states that chromatic adaptation can be thought of as the independent gain regulation of cone related sensors. Often sensor primaries are used that are sharper than the cone fundamentals themselves. However, although significant differences exist in many cases, it was shown that, compared to the impact of other model specifics, the corresponding prediction errors are quite small.

The simple one-step and two-step von Kries CATs with freely optimized degrees of adaptation provided the lowest prediction errors. The worse performance of the other von Kries models and RLAB can be attributed to an overestimation of the effective degree of adaptation of the average observer. The non-linear models also had lower performance, but the reasons are more ambiguous. Substantial differences in performance of the models were found between corresponding color subsets composed of only neutral illuminations conditions and those that also contained non-neutral ones. This can be explained by the observation that the effective degree of adaptation of an observer drops as the color of the illumination becomes more chromatic and that the models fail to (correctly) account for this effect. Similar trends were observed when the model performance was tested using corresponding color data sets from literature, although the trends were less pronounced.

The optimized degree of effective adaptation for the two-step von Kries CAT was modelled by a bivariate Gaussian in a log-compressed Macleod-Boyton type chromaticity diagram. A von Kries CAT incorporating the modelled $D_{eff}$ was found to provide low prediction errors for the corresponding memory color data sets. An analysis of the experimental $D_{eff}$ showed that even for neutral illumination conditions $D_{eff}$ is lower than what would be expected from the high luminance background adopted in this study. Although the dark surround adopted is one possible cause, other appearance effects could have contributed as well. Low degrees of effective adaptation or discounting-the-illuminant have also been found in color constancy studies when observers had to make color

Optics EXPRESS

appearance matches (as they did in the memory color matching experiments) rather than surface color matches [8, 37]. The analysis also indicated possible interactions between object color and background color signaling possible contributions of simultaneous contrast to the memory color appearance matches, which will be explored in future studies

As a chromaticity dependent degree of chromatic adaptation is currently missing in many CATs and color appearance models, as well as a model for simultaneous color contrast, the results of this study (and future ones including more adapting luminance levels and simultaneous color contrast) could be used to provide further improvements to these models.

Optics EXPRESS

## Appendix A

**Table 1. Summary details of several corresponding color data sets from literature. (Lw = luminance of a perfect white reflector; Yb: background luminance factor; Medium: R = reflective, T = transmissive, M = monitor; Sample size: S = small, L = large; Method: Hap. = halscopic matching, Mem. = memory matching, Mag. = magnitude estimation)**

| | | Light sources | | Lw (cd/m²) | | | | | |
|---|---|---|---|---|---|---|---|---|---|
| Data set | Number of samples | Ref | Test | Ref | Test | Yb (%) | Medium | Sample size | Method |
| CSAJ-C | 87 | D65 | A | 1000 | 1000 | 20 | R | S | Hap. |
| Kuo & Luo (A) | 40 | D65 | A | 1068 | 1068 | 16 | R | L | Mag. |
| Kuo & Luo (TL84) | 41 | D65 | TL8 | 1068 | 2293 | 12 | R | S | Mag. |
| Lam & Rigg | 58 | D65 | A | 1170 | 1000 | 20 | R | L | Mem. |
| Helson | 59 | D65 | A | 785 | 613 | 21 | R | S | Mem. |
| LUTCHI (A) | 43 | D65 | A | 763 | 729 | 20 | R | S | Mag. |
| LUTCHI (D50) | 44 | D65 | D50 | 763 | 792 | 20 | R | S | Mag. |
| LUTCHI (WF) | 41 | D65 | WF | 763 | 792 | 20 | R | S | Mag. |
| Breneman-C | 12 | D65 (D60 | A | 5000 | 5000 | 30 | T | S | Hap. |
| Breneman-C | 12 | D55 | P | 5200 | 5200 | 30 | T | S | Hap. |
| Breneman-C | 12 | D55 | P | 260 | 260 | 30 | T | S | Hap. |
| Breneman-C | 12 | D65 | A | 260 | 260 | 30 | T | S | Hap. |
| Breneman-C | 11 | D55 | A | 3875 | 3875 | 30 | T | S | Hap. |
| Breneman-C | 12 | D65 | A | 1220 | 1220 | 30 | T | S | Hap. |
| Breneman-C | 12 | D65 | A | 50 | 50 | 30 | T | S | Hap. |
| Breneman-C | 12 | D65 (D70 | A | 5450 | 5450 | 30 | T | S | Hap. |
| Breneman-C | 12 | G | D55 | 260 | 260 | 30 | T | S | Hap. |
| Braun & Fairchild | 17 | D65 | D95 | 129 | 129 | 20 | M to R | S | Hap. |
| Braun & Fairchild | 16 | D65 | D95 | 129 | 129 | 20 | M to R | S | Hap. |
| Braun & Fairchild | 17 | D65 | D30 | 129 | 129 | 20 | M to R | S | Hap. |
| Braun & Fairchild | 16 | D65 | D30 | 129 | 129 | 20 | M to R | S | Hap. |
| McCann | 17 | D35 (N) | D35 (N) | 24 | 24 | 30 | R | S | Hap. |
| McCann | 17 | D65 | R | 25 | 25 | 30 | R | S | Hap. |
| McCann | 17 | D65 | Y | 33 | 33 | 30 | R | S | Hap. |
| McCann | 17 | D35 | G | 40 | 40 | 30 | R | S | Hap. |
| McCann | 17 | D65 | B | 14 | 14 | 30 | R | S | Hap. |

Optics EXPRESS

## Appendix B

**Table 4. Prediction errors in terms of $DE_{u'v'}$, $DE^*_{ab}$ and DE*00* for the von Kries models using the CAT02 sensor space for the corresponding memory color data sets and those from literature.**

| | Memory color sets | | | | | | Literature sets | | | | | |
|---|---|---|---|---|---|---|---|---|---|---|---|---|
| Model #: | 1 | 2 | 3 | 4 | 5 | 6 | 1 | 2 | 3 | 4 | 5 | 6 |
| Model description: | von Kries, $D_{1,2}$ = opt. (2-step: A to EEW to B) | von Kries, $D_1$ = opt. (1-step: A to B) | von Kries $D_{1,2}$ = 1 (2:step: A to EEW to B) | von Kries, $D_{1,2} = D_{CAT02}$ (2-step: A to EEW to B), | von Kries, $D_{1,2} = D_{cmccat2000}$ (2-step: A to EEW to B) | von Kries, $D_{1,2} = D_{ccmccat97}$ (2-step: A to EEW to B) | von Kries, $D_{1,2}$ = opt. (2-step: A to EEW to B) | von Kries, $D_1$ = opt. (1-step: A to B) | von Kries $D_{1,2}$ = 1 (2:step: A to EEW to B) | von Kries, $D_{1,2} = D_{CAT02}$ (2-step: A to EEW to B), | von Kries, $D_{1,2} = D_{cmccat2000}$ (2-step: A to EEW to B) | von Kries, $D_{1,2} = D_{ccmccat97}$ (2-step: A to EEW to B) |
| | ***All corresponding color data sets*** | | | | | | | | | | | |
| **DE*u'v'*(1e-3)** | 3.8 | 5.2 | 38.3 | 28.1 | 38.3 | 28.1 | 8.0 | 7.8 | 11.1 | 9.6 | 10.7 | 9.6 |
| **DE*ab** | 3.7 | 4.7 | 32.2 | 24.3 | 32.2 | 24.3 | 5.3 | 4.8 | 6.3 | 5.9 | 6.1 | 5.9 |
| **DE*00*** | 2.0 | 2.7 | 11.8 | 9.1 | 11.8 | 9.1 | 3.1 | 2.9 | 3.5 | 3.2 | 3.4 | 3.2 |
| | ***Neutral to neutral only (CCT ≥ 3500 && CCT ≤ 10000 && \|Duv\| ≤ 0.015 for both illuminations conditions)*** | | | | | | | | | | | |
| **DE*u'v'*(1e-3)** | 2.2 | 2.4 | 8.0 | 5.3 | 8.0 | 5.3 | 7.3 | 7.4 | 9.0 | 8.0 | 8.3 | 7.7 |
| **DE*ab** | 2.0 | 2.2 | 6.2 | 4.1 | 6.2 | 4.0 | 4.2 | 4.3 | 5.3 | 4.6 | 4.7 | 4.5 |
| **DE*00*** | 1.1 | 1.3 | 2.6 | 1.8 | 2.6 | 1.8 | 2.5 | 2.7 | 3.1 | 2.7 | 2.8 | 2.7 |
| | ***Non-neutral to non-neutral (CCT < 3500 && CCT > 10000 && \|Duv\| > 0.015 for both illuminations conditions)*** | | | | | | | | | | | |
| **DE*u'v'*(1e-3)** | 4.1 | 5.5 | 41.6 | 30.2 | 41.6 | 30.2 | 8.3 | 8.6 | 12.6 | 10.2 | 11.0 | 10.2 |
| **DE*ab** | 3.9 | 4.9 | 34.1 | 25.4 | 34.1 | 25.4 | 6.0 | 5.6 | 6.8 | 6.1 | 6.7 | 6.1 |
| **DE*00*** | 2.1 | 2.7 | 12.4 | 9.8 | 12.4 | 9.7 | 3.3 | 3.2 | 3.8 | 3.4 | 3.6 | 3.4 |
| | ***Neutral to non-neutral*** | | | | | | | | | | | |
| **DE*u'v'*(1e-3)** | 3.6 | 4.3 | 32.6 | 21.8 | 32.6 | 3.6 | 6.1 | 5.9 | 8.5 | 7.7 | 8.1 | 7.1 |
| **DE*ab** | 3.3 | 3.5 | 27.8 | 20.2 | 27.8 | 3.3 | 4.5 | 4.2 | 6.1 | 5.3 | 5.3 | 5.3 |
| **DE*00*** | 1.8 | 1.9 | 10.1 | 7.6 | 10.1 | 1.8 | 2.5 | 2.4 | 3.0 | 2.6 | 2.9 | 2.5 |
| | ***Non-neutral to neutral*** | | | | | | | | | | | |
| **DE*u'v'*(1e-3)** | 3.3 | 4.2 | 41.0 | 29.3 | 41.0 | 3.3 | 9.5 | 9.1 | 11.3 | 10.2 | 10.7 | 10.3 |
| **DE*ab** | 3.5 | 3.8 | 30.1 | 23.5 | 30.1 | 3.5 | 5.0 | 4.8 | 6.5 | 5.8 | 5.9 | 5.9 |
| **DE*00*** | 1.9 | 2.1 | 12.2 | 9.2 | 12.2 | 1.9 | 3.0 | 3.0 | 3.8 | 3.5 | 3.8 | 3.4 |

## Funding

Author KS was supported through a Postdoctoral Fellowship of the Research Foundation Flanders (FWO) (12B4916N). And QZ by a grant of the International Fund KAHO Sint-Lieven, call 2015.